Available online at www.CivileJournal.org

Civil Engineering Journal

(E-ISSN: 2476-3055; ISSN: 2676-6957)

Vol. 12, No. 03, March, 2026

Evaluating Micro-Crack Propagation in Concrete Under Freeze-Thaw Cycles Using a Multi-Frequency Ultrasonic Approach

Sabah H. Fartosy [1*], Mithaq Kohees [2], Zubaidah A. Mohammed Ali [3], Jinan M. Faleeh [2], Salah Hassan [2]

[1] *Department of Water Resources Engineering, College of Engineering, Mustansiriyah University, Baghdad, 10047, Iraq.*

[2] *Department of Civil Engineering, Mustansiriyah University, Baghdad, 10047, Iraq.*

[3] *Building and Project Management Engineering Department, Al-Esraa University, Baghdad, Iraq.*

Received 16 May 2025; Revised 27 January 2026; Accepted 04 February 2026; Published 01 March 2026

Abstract

Concrete is a widely used construction material that degrades over time for various reasons, meaning an integrity assessment is necessary for concrete to ensure it performs as expected for design requirements. This research employs velocity and attenuation of ultrasonic wave propagation to evaluate the development of micro-cracking in a concrete medium subjected to freezing and thawing. Four concrete cylinder samples were cast from an air-entrained admixture with various percentages of aggregate. Conventional Ultrasonic Pulse Velocity (UPV) testing was performed with three pairs of transducers (54 kHz, 250 kHz, and 500 kHz) on the specimens undergoing temperature cycling. Two methods of comparative analysis evaluated the relationship between inherent characteristics of the propagated waves and the induced development of cracks in the specimens. Results from the comparative analyses indicate that transducer frequency plays an important role in the accuracy and specificity of non-destructive testing (NDT) assessments. 54 kHz provides a more generic assessment of macro-scale deterioration; however, higher frequencies, and specifically 500 kHz, provide a level of detail that renders optimal air-entrained percentages distinguishable and freeze-thaw tested concrete's internal cracking development discernible with greater certainty. These results strongly support NDT testing of concrete for durability considerations with advanced blends in cold exposure regions. Such varying frequencies allow concrete stakeholders to appreciate global trends in addition to localized damage attributes for effective assessments of material capability and service life predictions.

Keywords: Wave Attenuation; Concrete Medium; UPV; Freeze-Thaw Cycles; Crack Propagation.

1. Introduction

The properties of concrete constituents are among the most critical parameters that impact damage development within a concrete medium as a behavior, for many reasons. Cracking concrete members are subjected to external loads, chemical transformations within concrete due to aggressive chemicals, and volumetric growth due to different temperature variation cycles [1-3]. In addition, under sufficient conditions, the development of microcracks within concrete material allows extensive crack development [4-7]. The influence of micro to macro cracks under certain conditions substantiates the need for reliable detection means before concrete failure occurs during this transition. While a few means of nondestructive testing (NDT) approaches have been implemented for the detection of crack occurrences in concrete elements [8-11]—UPV, visual inspection, acoustic emission, microscopy, and resonant frequency—no

* Corresponding author: dr.sabah77@uomustansiriyah.edu.iq

https://doi.org/10.28991/CEJ-2026-012-03-017

significant and reliable detection means of microcracks generated internally within concrete due to externally and internally induced reactions exists. NDT has, however, sufficiently noted crack growth occurrence amassed in a concrete medium as a result of testing due to expansive cycles of temperature variations. For example, an ultrasonic pulse velocity (UPV) test, pulse echo, has been extensively utilized by engineers as the concrete integrity condition assessment tool that addresses and justifies crack growth. The UPV principle is a combination of two ultrasonic transducers set at 54 kHz, with one penetrating with a pulse from one side and the other receiving the response from the other side. By knowing the distance and the time of travel, a wave velocity can be calculated. This is subsequently utilized for characterization of the tested materials. Unfortunately, many researchers claim that UPV as is does not adequately depict damage linked to micro-cracking from internal ice growths [12-14]. Furthermore, many researchers claim that both relative wave velocity and crack growth cannot be measured below half the length of the wavelength [15, 16]. Therefore, taking wave attenuation into consideration as a secondary ultrasound parameter offers a more reliable detection means of small cracks developed within concrete due to both NDT and temperature variation cycles.

Many researchers assessed the impact of temperature variation cycles (freeze-thaw) on the mechanical properties of concrete, analyzing strength, deformation magnitude, and stiffness [17-21]. Various methods were attempted to mitigate the consequences on concrete performance and durability post repeated cycles of freeze-thaw, such as air-entrained admixture, prolonged curing time, and reduced water-cement ratio [22]. Air-entrained admixture was the most frequently linked material due to its apparent support for concrete durability against frost impact [23-24]. This is justified with recent findings that UPV cannot distinguish between damage induced internally and damage induced externally [25]. This is corroborated by disparate readings due to admixture contributions; Zalegowski [26] found that while AER supports improvement for frost resistance, it inherently lessens ultrasonic velocity naturally. In addition, these environmental attacks are often compounded; F-T cycles, F-T, and other ingressions create additive deterioration [27].

Several researchers evaluated the effectiveness of varying percentages of air-entrained additives (0.1 to 0.5) in the concrete mixture under freeze-thaw applications. These studies found concrete significantly more resilient after freeze-thaw cycles due to the incorporation of air-entrained additions. Therefore, in accordance with findings from the literature, four percentages (0.00%, 0.100%, 0.150%, and 0.250%) per cement-mass weight of air-entrained additive were integrated into the concrete materials to evaluate the impact of air-entrainment on small crack occurrence within the concrete medium [26-30].

The purpose of this study is to assess the difference between varied air-entrained percentages in NDT performance for crack occurrence before and after freeze-thaw application. Therefore, four cylinders were cast with different air-entrained additives (0%, 0.1%, 0.15%, and 0.25%) and conventionally UPV tested before and after established freeze-thaw cycles. In addition, ultrasonic testing was conducted against three types of ultrasonic transducers (54 kHz, 250 kHz, and 500 kHz) to assess frequency correlation and crack establishment. Two data assessments were taken: one relying on the physicalness of wave velocity measurement and one relative assessment based on an assessed assessment of attenuation due to ultrasonic wave particle current due to small cracks created from cylinder sample formation based on amplitude peaks and frequency spectrum analysis. Ultimately, both wave velocity and attenuation were taken as final assessment means to determine true relationship dynamics between propagated wave signals and accumulated microcracks developing in concrete samples as a function of temperature variation cycles.

The structure of the paper is as follows. Section 2 details the testing method, from specimen fabrication to the setup of the freeze-thaw machine to UPV testing. Section 3 presents the results with discussion relative to crack growth based on wave velocity, time-domain response, and frequency domain response. Finally, Section 4 lists the results observed and final thoughts of the experiment.

2. Testing Methodology

2.1. Specimen Fabrication

Four concrete cylinder specimens (10.0 × 20.0 cm) are produced using the specified design mixture proportions, including air-entrained agent (Sika manufactured), as seen in Table 1. In the constituents of concrete mixing proportions, four different air-entrained percentages are present using casting (0.00%, 0.100%, 0.125%, and 0.250%) of the cement mass. Concrete mixing proportions are based on ACI Code [31]. Furthermore, the mixtures are made of Portland ASTM (type-I) cement, fine and coarse aggregates with a nominal aggregate size of 12.50 mm, and a water/cement ratio of 40% by mass. Furthermore, the specified proportions for the designed concrete are a 35.0 MPa compressive strength at 28.0 days and a workability slump of 75.0-100.0 mm.

Table 1. Details of mix proportions of concrete samples

Specimen No.	AE-agent* (%)	Cement. (kg/m^3)	Fine-agg. (kg/m^3)	Coarse-agg. (kg/m^3)
Cy1-Cy4	0, 0.1, 0.125, 0.25	520	705	992

* Air-entrained additive.

2.2. Freeze-thaw Equipment Details

A commercial small-size freezer is adjusted to be used as a control chamber to produce temperature variation cycles (freeze and thaw) as shown in Figure 1. The freezer is supplied with an electric heater placed inside to raise the temperature value to the specified level through the thawing process. An electrical switch timer wired to the operational switch for the freezer and heater is adjusted to 8.0 hours needed to freeze and 14.0 hours needed to thaw. Thus, to replicate a freeze-thaw cycle of accelerated 1 day (24.0 hours), the steady temperature change is facilitated and adjusted to slowly increase from -25.0°C to +25.0°C with ± 2.0°C. All concrete specimens are kept inside the freezer and continuously subjected to the freeze-thaw cycle for eight weeks.

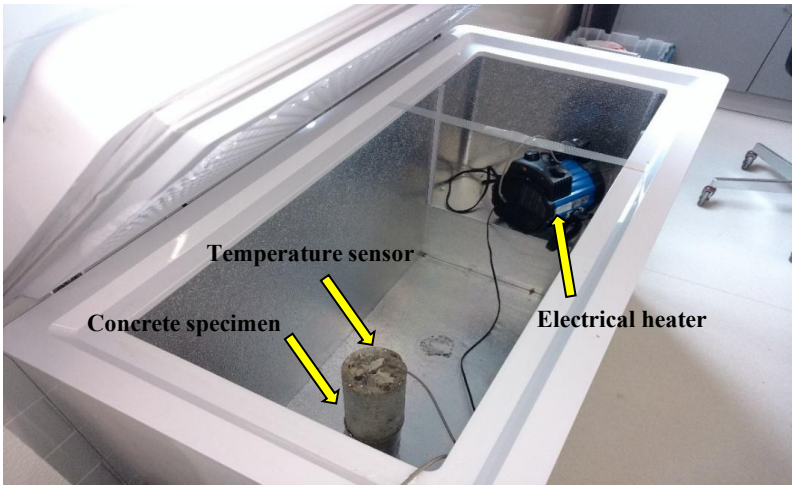

Figure 1. Adjusted commercial small-freezer to simulate cycles of freeze-thaw

2.3. Ultrasonic Pulse Velocity (Setup and Procedure)

The configuration of the UPV testing setup consists of the following components: digital oscilloscope to capture signals, function generator to produce wave signals, ultrasonic transducers to emit and receive signals through concrete specimens, piezo driver, and Laptop computer to save and process the testing data as shown in Figure 2.

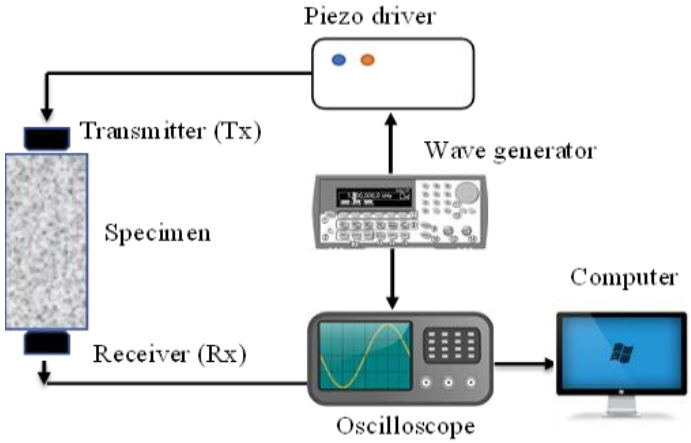

Figure 2. The configuration of the UPV testing instrument used in testing concrete specimens

Three pairs of ultrasonic transducers are employed with nominal frequencies (54.0 kHz, 250 kHz, and 500.0 kHz) dedicated to UPV measurement. UPV readings are registered before and after the temperature fluctuation aging of concrete samples. In addition, a gel is applied between each ultrasonic transducer and the surface of the tested samples to ensure coupling efficiency and reduce signal loss during transmission [32]. Moreover, three 3D-printed holders with rubber bands are designed for a fixed holding position for UPV testing to maintain proper coupling of transducers on the tested samples. This is shown in Figure 3.

All concrete samples are kept in a water tank for (4) days before freezing and thawing cycles are applied, and once applied, they are resubmerged to further the temperature variations. Then UPV measurements are taken post-tank removal. Thereafter, all concrete samples are tested within an 8-week time frame. The two analysis methods

determine the correlation between the frequency content relative characteristics of the propagated ultrasonic wave and the subsequent cracking formation in concrete samples exposed to repeated freeze-thaw cycles in succession over time.

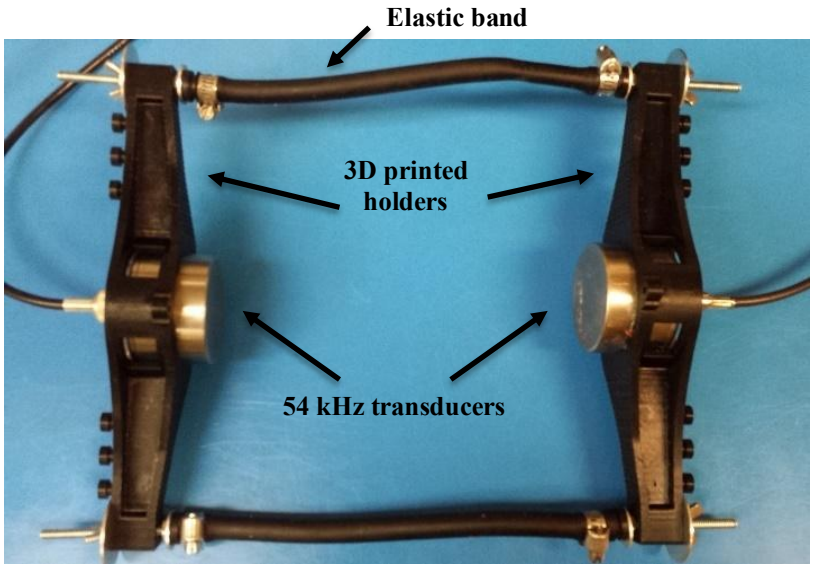

Figure 3. Typical 3D printed 54 kHz transducer holders with elastic bands

The first method is the traditional ultrasonic wave velocity assessment method for predicting velocity of the wave based on temperatures induced cracking formation from temperature deviation cycles. The second method applies two approaches from the analysis of wave attenuation based on time and frequency. The first approach establishes wave attenuation ($A_{att.}$) from time relative characteristics of the received signals (peak amplitude) and before and after eight weeks of freeze-thaw cycles using Equation 1 [33]:

$$A_{att} = 20\,log_{10}\frac{Amp_0(t)}{Amp_d(t)} \quad (1)$$

where, A_{mpo} and A_{mpd} are the peak-to-peak wave amplitudes before and after freeze-thaw cycles. Then, in the second approach, the area under the spectrum frequency is used to calculate wave attenuation before and after freeze-thaw cycles. Eq. 1 is also used by replacing S_{p0} (area of signal spectrum before) and S_{pd} (area of signal spectrum after)

2.4. Theoretical Basis of Multi-Frequency of UPV

The underlying theory behind ultrasonic pulse velocity (UPV) testing of concrete comes from wave propagation for non-destructive testing (NDT). The velocity in which the ultrasonic wave propagates depends upon the elastic modulus and density of the propagation medium. However, where the propagation medium comprises discontinuities, pores and micro-cracks, for example, the propagation velocity will vary. The second theoretical component that underlies the study comes from the relationship between wavelength (λ) and defect/dimension of interest (d). This relationship defines to what extent a measurement can be defect sensitive:

- λ >> d: The wavelength is larger than that of the micro-crack, and the wave diffracts around the defect, losing some energy but maintaining velocity in a way, "losing" the defect in the crack. This is the response from low frequency transducers (54 kHz) that can measure a more generalized, macroscopic characteristic of concrete.
- λ ≈ d: The wavelength on the order of the defect results in a defect scattering and attenuation of significant order, in other words, the crack does not matter as much because the wave is now at a similar wavelength interacting with it but with great attenuation of the amplitude/velocity of measured signal.
- λ < d: The wave is so small it perceives the crack as a separate reflector, with much better resolution capacity.

In this case, these micro-cracks are expected to be the result of freeze-thaw cycles. Low frequency (54 kHz) waves produce long wavelengths and are generally insensitively toward this early micro-damage. On the other hand, high frequency (250 kHz and 500 kHz) waves produce much smaller wavelengths than the 250 kHz waves expected to be more sensitive to scattering associated with these small initiating micro-cracks. Thus, it should be possible to distinguish between bulk/micro-damage through response at varying frequencies. Figure 4 shows the methodology that followed in this study to conduct the testing procedure.

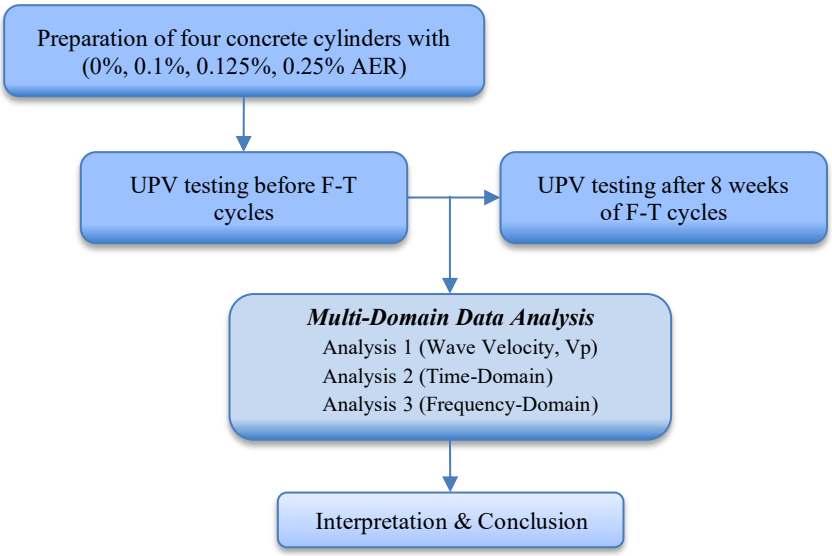

Figure 4. Flowchart of the testing methodology

3. Results and Discussion

3.1. Wave Velocity Interaction with Small Cracks

Ultrasonic Pulse Velocity (UPV) readings of the four cylindrical samples (Cy1-Cy4) were taken before and after eight weeks of freeze-thaw cycling to gauge their wave propagation characteristics. The measured wave velocities can be seen in Figure 5, while Table 2 exhibits these data points and their respective standard deviations (*Std*). These readings were taken at nominal frequencies of 54 kHz, 250 kHz and 500 kHz. Specifics of Figure 5 and Table 2 reveal an inherent limitation of the P-wave velocity (*Vp*) as a diagnostically useful measurement in the current study. For example, the most baseline samples do not exhibit consistent or monotonic change with the increasing number of freeze-thaw cycles when assessed at each frequency, in addition to minimal readings and in some cases, below measurement uncertainty (standard deviation). What this means is that there is no statistically significant change due to the observed values being too close to one another.

Table 2. Average velocities of all tested concrete specimens.

Specimen no.	AE-agent* (%)	54 kHz		250 kHz		500 kHz	
		V_p (m/s)	Std (±)	V_p (m/s)	Std (±)	V_p (m/s)	Std (±)
Cy1	0	4745	35	4879	82	4825	74
Cy2	0.1	4849	40	4837	49	4878	48
Cy3	0.125	4630	40	4528	155	4838	73
Cy4	0.25	4624	34	4757	27	4763	32

*Air-entrained additive.

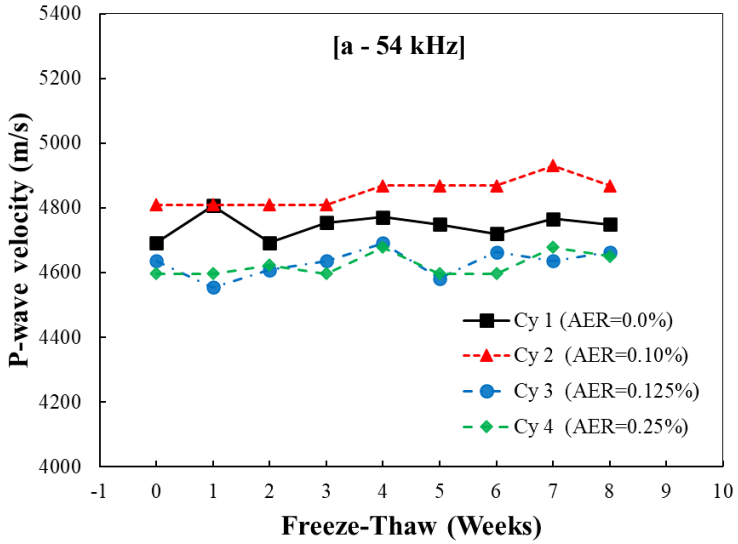

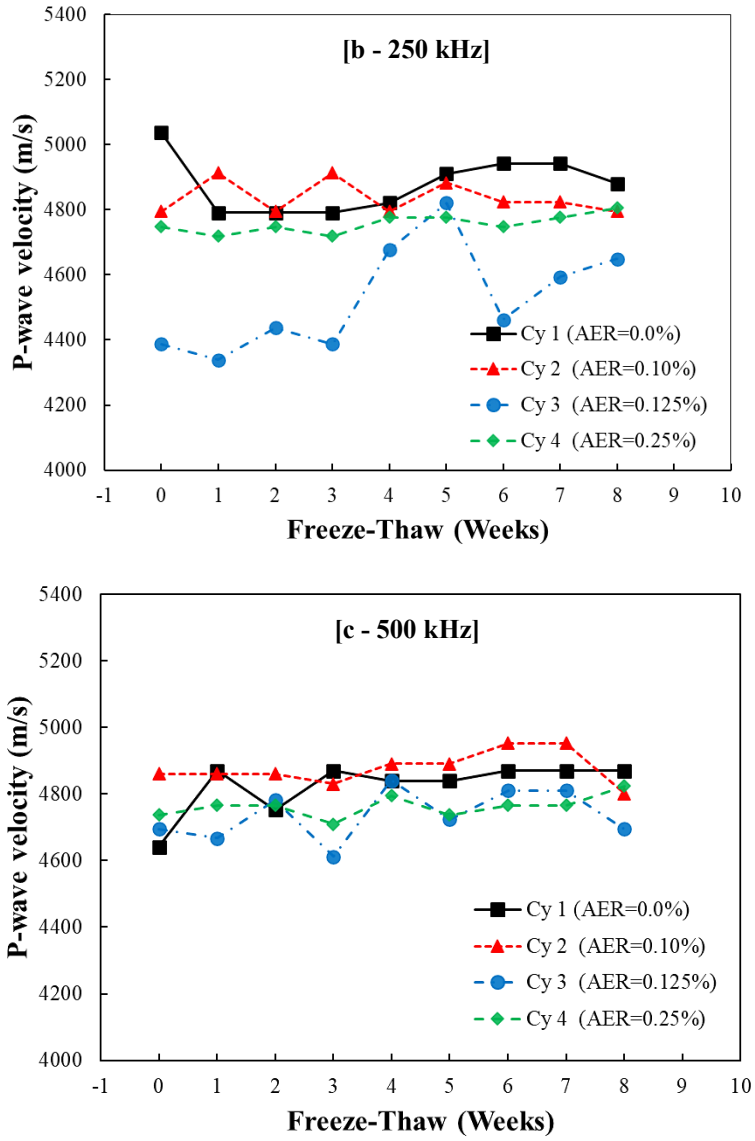

Figure 5. Wave velocities after testing cylinder concrete samples contained different ratios of air entrained admixture, a) using a 54 kHz transducer, b) using a 250 kHz transducer, c) using a 500 kHz transducer

Such an insensitivity is, however, of a curious nature, as well. Since velocity is determined from elastic modulus and density, observing the P wave velocity and minimal lack thereof indicates that microcracking induced by eight weeks of constant, winter-like exposure is either too small, too sparse or too inadequately connected to require a significant measurement decrease of concrete's macro elastic modulus. In fact, since ultrasonic P-waves (especially lower frequency ones) can diffract around microscale imperfections, they can travel expediently through a largely consolidated matrix.

Therefore, effective travel time remains uniform for wave propagation with this slight change - deeming *Vp* an insensitive parameter at the early damage onset stage. This Vp independence was felt at all three frequencies tested (54, 250, 500 kHz) during this early damage onset stage. Therefore, where wave velocity is concerned, it is clear that until significant levels of cracking are present to assess growth via reflection/attenuation thresholds that cracking that is developed through freeze thaw temperatures is futile as a means of assessing this onset. Therefore, it is necessary to determined assess a complementary parameter that is more sensitive to changes in microstructure. Thus, what will be assessed next is wave attenuation behavior.

3.2. Crack Detection in the Time Domain

While wave velocity (*Vp*) showed relative insensitivity to levels of frost damage incurred during the formative stage of fracture, *Vp* results on wave attenuation indicate a much more attenuated and quantifiably sensitive measure of damage comparison for internal damage. For example, attenuation, energy amplitude and strength of a signal receiving transducer over distance, is not relative to the bulk elastic modulus (like *Vp*) but instead, to scattering absorption of energy. Microcracks, voids, and discontinuities create more internal surfaces that scatter/transmit ultrasonic energy in addition to dissipating it attenuation for effectively reducing the energy that received at the sensor. Thus, attenuation proves to be an effective surmising measure of incipient microstructural damage that has not yet developed into obvious, visible external cracks.

Results at 54 kHz (Low Frequency - Low Resolution)

Figure 6 shows the time domain readings received by the 54 kHz transducer heads. There was an (82%) loss of signal energy as compared to the input reading for the non-air-entrained specimen (0% AER). In contrast, (60-65%) loss values were reported for all air-entrained specimens (AER). This includes the protective capacity of air entrainment against frost damage. The 0% AER sample had no pressure relief components and as a result, ice expansion microcracking was extensive. The ice expansion that created new surfaces now surfaces that are cracks increased scattering of the 54 kHz energy and, consequently, much more energy was lost. The air bubbles within the AER mixtures provided a networking component of microscopic holes that absorbed the volume expansion during the freezing and thus, created fewer microcracks, which developed lower energy reductions to attenuation.

Note that there is a statistical insignificance between all percentages of air-entrained specimens (0.1%, 0.125%, 0.25% AER). This does not mean they are of the same damage level but that the transducer is low resolution and the 54 kHz wavelength (λ_{54} = 8.0 cm) cannot differentiate the subtle variations between these three high-performing mixtures in terms of micro-damage or void distribution. It can only conclude that they are either "heavily damaged" or "protected".

Results at 250 kHz (High Frequency - Diagnostic Resolution)

As such, 250 kHz transducers were used to assess specimens to further push beyond spatial limitations of the 54 kHz tests. Figure 7 shows the results of such tests. In addition, for 0% AER there was a further (90%) loss in signal energy when compared to 54 kHz. The degree of loss was much higher than (82%). This means that the 250 kHz wave interacts with many smaller microcracks that 54 kHz cannot interact with to detect. The fact that it can obtain different readings for different frequencies is a well-established fingerprint of distributed micro-damage as opposed to localized micro-damage.

In fact, at this frequency, distinctions between AER levels begin to be detected. Specimen 3 (0.125% AER) experienced the least signal attenuation (≈64% reduction) with the most stability of waveform. While specimen 4 (0.25% AER) experienced greater attenuation (≈70%). This indicates there is an optimal air entrainment dosage. The formation/presence of microscopic holes acts as great preventative measures against frost damage when there are enough holes to present resistance but not so many as to compromise matrix integrity. The 0.125% AER specimen is the ideal air void system. The 0.25% AER specimen potentially has added air or over-entrainment as its holes compromised matrix integrity due to increased volume yet insufficient air bubbles in the better mixes. However, this would likely go undetected until a proper frequency resolution was used to assess microdamage.

Results at 500 kHz (Very High Frequency - High-Sensitivity Confirmation)

Results at 500 kHz (λ_{500} = 1.0 cm) provided the highest spatial resolution of any test conducted (Figure 8). Similarly, for the non-air-entrained specimen, there was (96%) signal reduction confirmed again for this highest frequency tested. In addition, the consistent signal drop confirmed through multiple assessments (82% → 90% → 96%) is reliable with a sample that determines what damage was sustained, i.e., as the wavelength decreases, the ultrasonic wave interacts with many smaller faults where all findings yielded significant percent reductions in power.

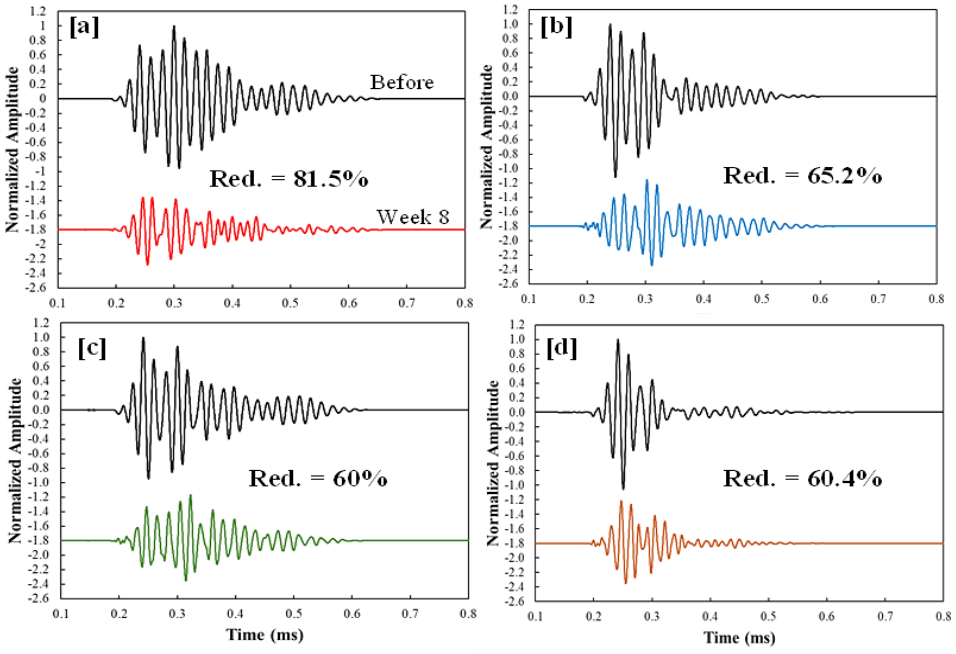

Figure 6. Wave signals obtained after testing concrete cylinders using a 54 kHz transducer, a) specimen 1 with 0% AER, b) specimen 2 with 0.1% AER, c) specimen 3 with 0.125% AER, d) specimen 4 with 0.25% AER

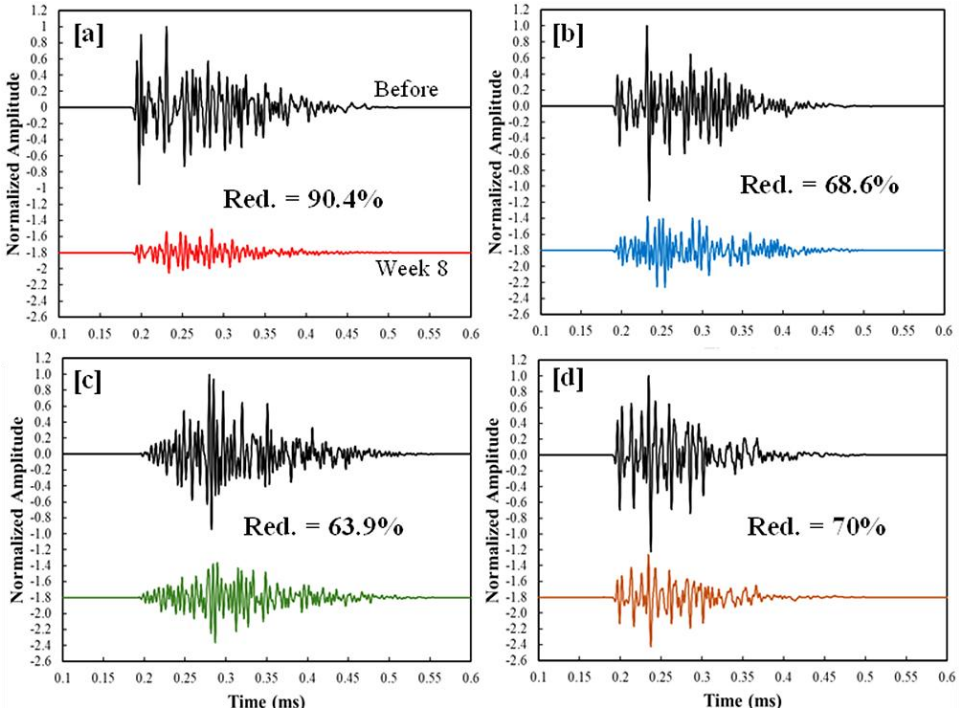

Figure 7. Wave signals obtained after testing concrete cylinders using a 250 kHz transducer, a) specimen 1 with 0% AER, b) specimen 2 with 0.1% AER, c) specimen 3 with 0.125% AER, d) specimen 4 with 0.25% AER

The final frequency confirms findings from the previous one. As expected, the air-entrained specimens outperformed the non-AER specimen with an energy reduction of (71-76%) received, slightly higher than what was experienced at 250 kHz (64-70%), as expected from the increased sensitivity in assessment with decreased wavelength. Specimen 3 (0.125% AER) had the lowest energy reduction, indicating it is the ideal mixture for exposure to frost damage. While specimen 4 (0.25% AER) held higher attenuation, consistent with the idea that the addition of air reduced cohesion within the confines of the matrix. Note that consistency across the spectrum from 250 kHz and even more so at 500 kHz, a robust reading, and the enhanced nature for frequency-dependent attenuation supported from all three tests confirm that attenuation is a much more sensitive indicator for incipient signs of frost damage than wave velocity values ever could ascertain as detected and quantified by microstructural damage before any significant cracks could form due to early exposure from freeze-thaw cycles.

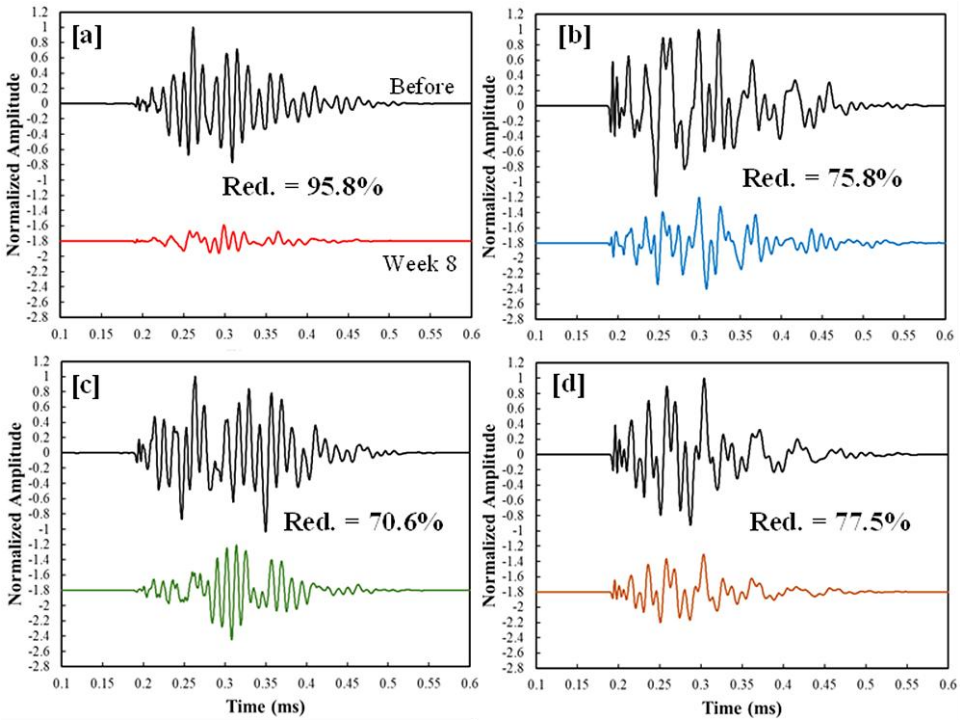

Figure 8. Wave signals obtained after testing concrete cylinders using a 500 kHz transducer, a) specimen 1 with 0% AER, b) specimen 2 with 0.1% AER, c) specimen 3 with 0.125% AER, d) specimen 4 with 0.25% AER

3.3. Crack Detection in the Frequency Domain

Whereas the time domain was more definitive in measuring total energy loss (attenuation), the frequency domain (Figures 9 to 11) is more of a diagnostic, nuanced finding as it reveals how the damage changes the frequency makeup of the wave instead of its total energy.

Spectral Area Confirms Attenuation Trends (Robust Confirmation)

Therefore, the area of the Fourier spectrum is merely a confirmation of the energy calculations found in the time domain which have clear merit.

- 54 kHz (Figure 9): The 0% AER sample lost (83%) of its spectral area while the AER protected samples only lost 55-62%.
- 250 kHz (Figure 10): The 0% AER sample lost (91%) of its spectral area while the protected samples only lost 66-74%.
- 500kHz (Figure 11): The 0% AER sample lost (96%) of its spectral area while the protected samples only lost 60-76%.

These figures perfectly mirror the loss in the time domain. They confirm the incremental, frequency-based attenuation (83% → 91% → 96%) as being attuned to the damage sustained by the sample, confirming that higher frequencies are more affected by micro damage. They additionally re-confirm that specimen (3) that contains (0.125% AER) consistently showing lower (decreased area loss) across all conferring frequencies is confirmed as the best mix.

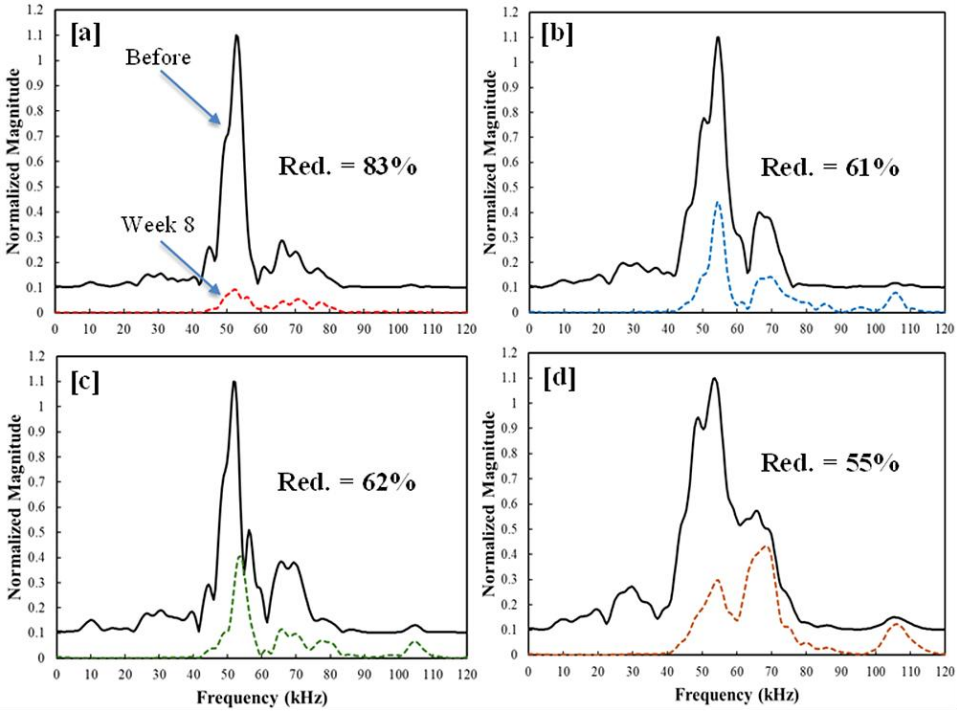

Figure 9. Wave frequency spectra results obtained after testing concrete cylinders using a 54 kHz transducer, a) specimen 1 with 0% AER, b) specimen 2 with 0.1% AER, c) specimen 3 with 0.125% AER, d) specimen 4 with 0.25% AER

Peak Shift Analysis (Diagnostic Finding)

The most significant and novel finding from spectral analysis relative to time was in the peak shift of the received signals. This is indicative of a physical manifestation in terms of what happens to the material at the micro level.

- 54kHz (Figure 9): An almost ubiquitous shifted peak occurred in the AER samples; thus, in Specimen (3) (the optimal sample); after 8 weeks of F-T cycles, it changed from 50kHz to 68kHz as a higher peak frequency.
- 250kHz (Figure 10): A more pronounced, diagnostically feasible event occurred here:
  - Specimen (1, 0% AER): Damaged sample peaked at 125kHz.

- Specimen (3, 0.125% AER): Good sample peaked at 200kHz.
- Specimen (4, 0.25% AER): Over-entrained sample dropped back to peak at 125kHz, the same as the damaged sample.

Thus, peak shifting is a classic example of how a material "filters" a wave. In this context, microdamage (such as cracks) and/or the air-void system itself act as a high-pass filter. Larger, disconnected flaws and voids are effective in scattering and attenuating low-frequency energy. In contrast, the intact and rigid portions of the concrete matrix provide a "fast path" that facilitates the transmission of higher-frequency components.

This means that, for specimen (3), the optimal sample, the shift in frequency up to 200 kHz is a positive indicator. It suggests that the concrete matrix is sufficiently dense and that the air-void system is well distributed, effectively filtering out lower frequencies while allowing higher-frequency energy (up to 200 kHz) to pass through. This indicates that the matrix remains intact and stiff. In contrast, samples (1) and (4), representing damaged and over-entrained conditions, respectively, exhibit peak frequencies at a lower value of 125 kHz, indicating matrix deterioration. In sample (1), the presence of cracks reduces the material's ability to transmit higher-frequency signals. In sample (4), excessive air content weakens the paste matrix, similarly preventing effective transmission of high-frequency energy.

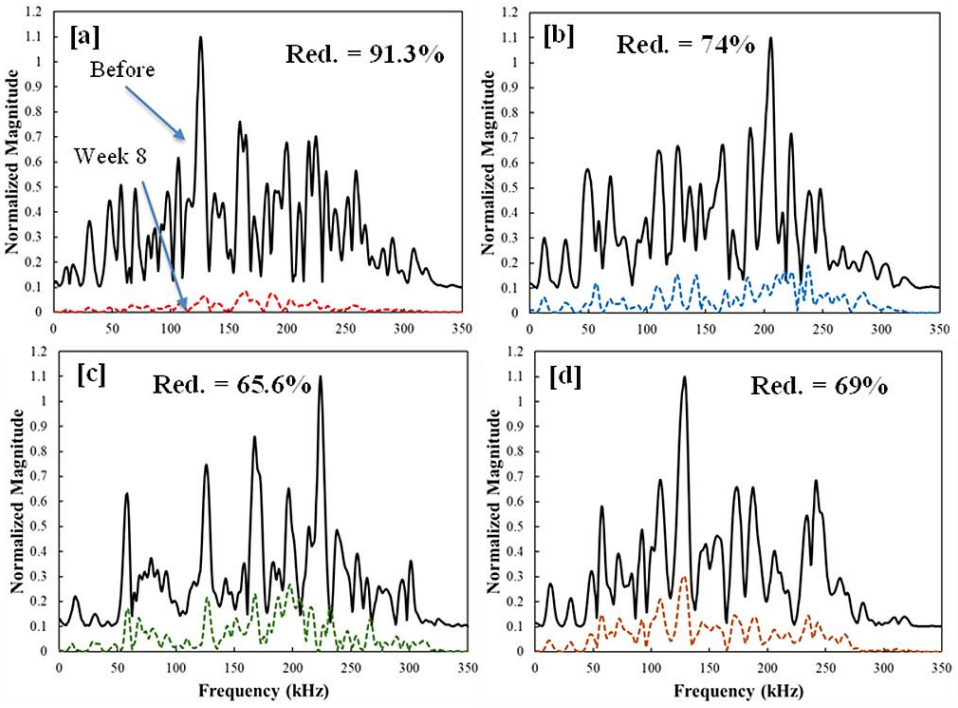

Figure 10. Wave frequency spectra results obtained after testing concrete cylinders using a 250 kHz transducer, a) specimen 1 with 0% AER, b) specimen 2 with 0.1% AER, c) specimen 3 with 0.125% AER, d) specimen 4 with 0.25% AER

Thus, the frequency domain adds a second level of critical corroborating evidence - whereas the area of the spectrum supports how much damage was done (attenuation), the shift involves diagnosing what's wrong with matrix integrity, successfully differentiating that over time, consensus is clear that the superior-in-integrity matrix exists at the 0.125% AER sample and no others.

3.4. Wave Attenuation Results

Figure 12 illustrates the calculated wave attenuation in decibels (dB), based on the peak amplitude of ultrasonic signals recorded from all concrete specimens before and after exposure to eight weeks of freeze-thaw cycles. The measurements are obtained using three different transducer frequencies: 54 kHz, 250 kHz, and 500 kHz, allowing for a comprehensive comparison of how frequency affects the detection of internal damage and the performance of air-entrained concrete (AER).

The results demonstrate that specimens containing various percentages of air-entrained admixture exhibit significantly lower wave attenuation compared to the non-air-entrained specimen (0% AER), confirming the effectiveness of AER in enhancing concrete durability under cyclic thermal stress. This trend was consistent across all tested frequencies, reinforcing the protective role of air bubbles in mitigating frost-induced microcracking and preserving the structural integrity of the concrete matrix.

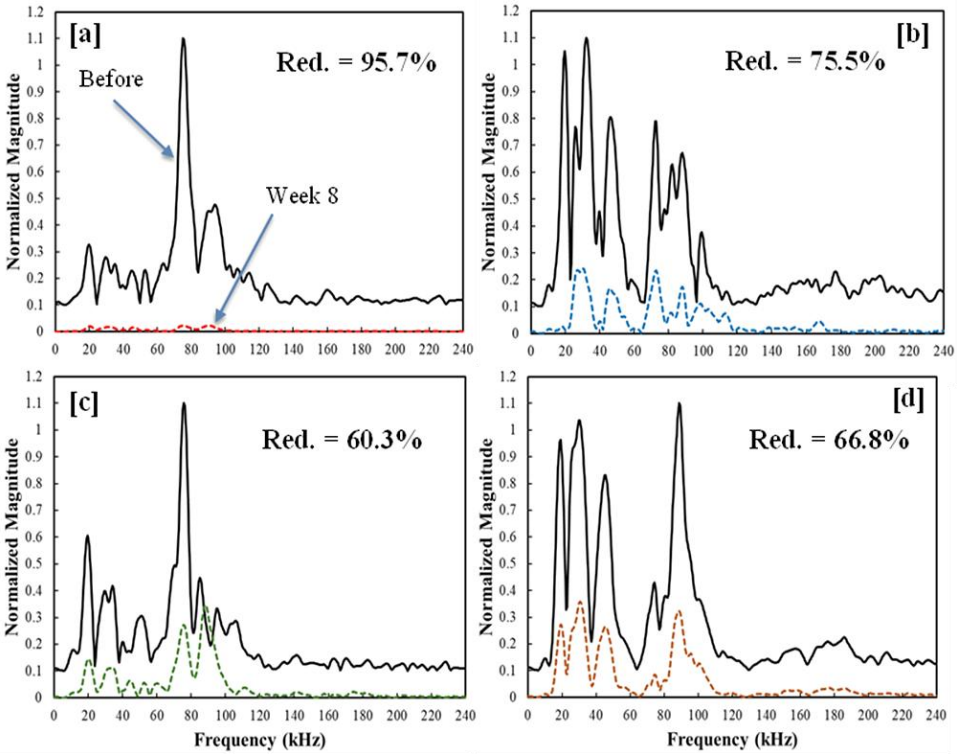

Figure 11. Wave frequency spectra results obtained after testing concrete cylinders using a 500 kHz transducer, a) specimen 1 with 0% AER, b) specimen 2 with 0.1% AER, c) specimen 3 with 0.125% AER, d) specimen 4 with 0.25% AER

However, a closer examination of the data reveals important differences in sensitivity among the transducer frequencies:

- At 54 kHz, while the general trend of improved durability with increasing AER dosage was observable, the results for all air-entrained specimens showed similar levels of attenuation, making it difficult to distinguish between concrete mixtures. This suggests that the longer wavelength ($\lambda 54$ = 8.0 cm) lacks the resolution necessary to detect fine-scale variations in internal damage or microstructural changes induced by different AER contents.
- In contrast, both 250 kHz and 500 kHz transducers provided much clearer differentiation between concrete mixtures. Specifically, Figures 12b and 12c (corresponding to 250 kHz and 500 kHz, respectively) highlight that a dosage of 0.125% AER yields the best performance in terms of minimizing wave attenuation and maximizing resistance to freeze-thaw damage. This finding aligns with earlier waveform analyses and further supports 0.125% as the optimal AER dosage for enhancing concrete durability under cyclic frost conditions.

Moreover, the results emphasize the frequency-dependent nature of wave attenuation in concrete. For instance, the non-air-entrained specimen (0% AER) exhibited the highest attenuation at 500 kHz (Aatt ≈18 dB), compared to ≈14 dB at 54 kHz and ≈16 dB at 250 kHz. This increase in attenuation with frequency confirms the superior sensitivity of higher-frequency transducers to early-stage microdamage, such as microcracking and debonding at the cement-aggregate interface, damage mechanisms that may remain undetected at lower frequencies.

While Figure 13 shows the calculated wave attenuation in decibels (dB), based on the area under the Fourier spectrum of ultrasonic signals obtained from testing concrete specimens before and after being subjected to eight weeks of temperature variation cycles. Also, the results revealed that specimens with air entrained agent (> 0% AER) exhibit significantly lower wave attenuation compared to the intact concrete specimen (0% AER), confirming the effectiveness of AER in enhancing concrete durability under cyclic thermal stress. This trend was consistent across all tested frequencies, reinforcing the protective role of air bubbles in mitigating frost-induced microcracking and preserving the structural integrity of the concrete matrix.

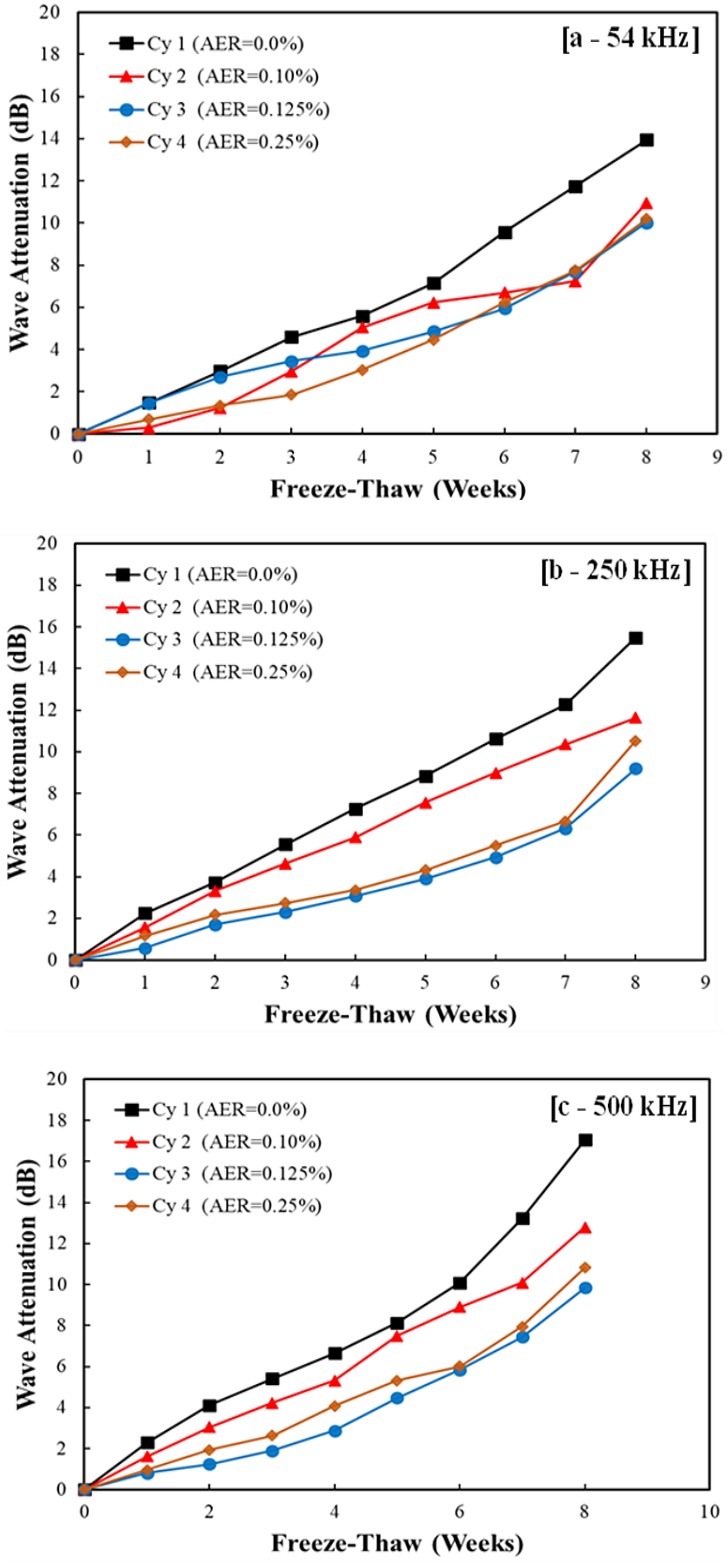

Figure 12. Wave attenuation based on peak amplitude of signals obtained after testing concrete cylinders, a) using 54 kHz, b) using 250 kHz, c) using 500 kHz

Moreover, the results emphasize the frequency-dependent nature of wave attenuation in concrete. For example, the concrete specimen with (0% AER) exhibited the highest attenuation at 500 kHz (Aatt≈17 dB), compared to ≈12 dB at 54 kHz and ≈14 dB at 250 kHz. This increase in attenuation with frequency underscores the superior sensitivity of higher-frequency transducers to early-stage microdamage, such as microcracking and debonding at the cement-aggregate interface, damage mechanisms that may remain undetected at lower frequencies.

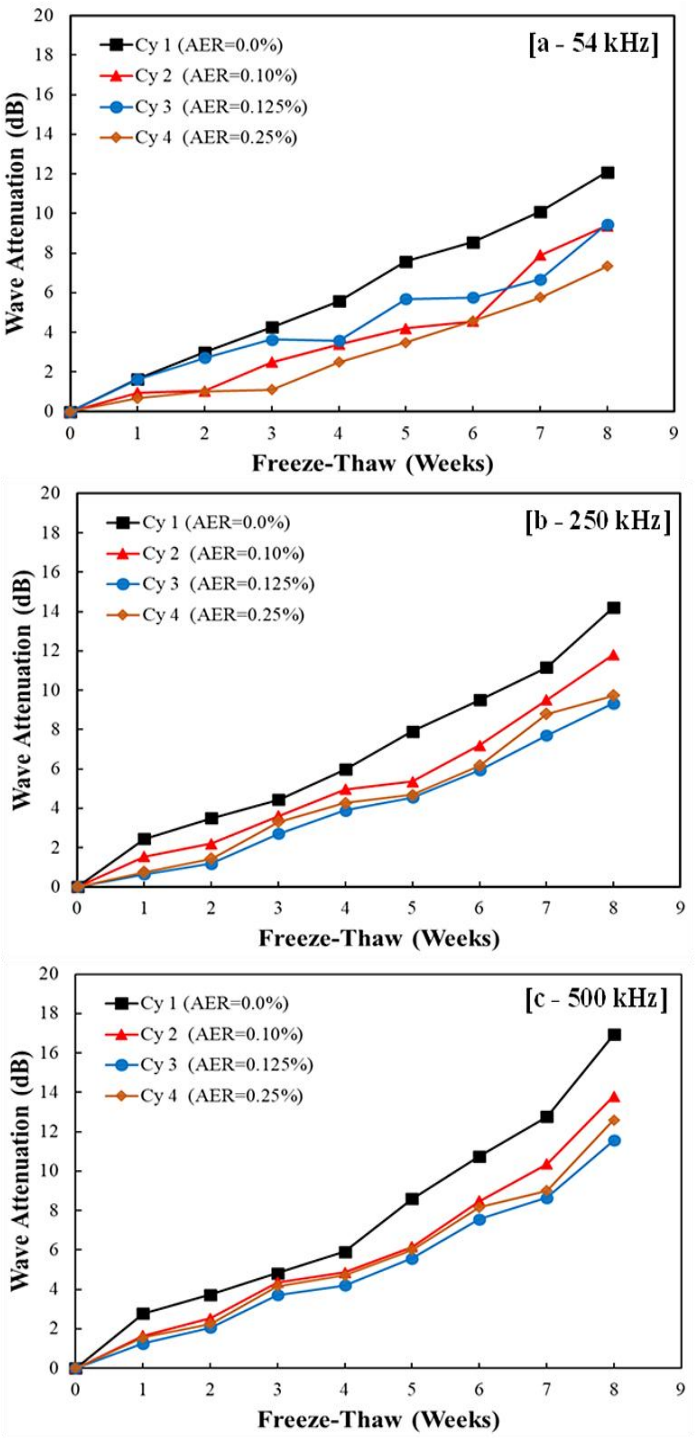

Figure 13. Wave attenuation based on frequency spectrum area of signals obtained after testing concrete cylinders, a) using 54 kHz, b) using 250 kHz, c) using 500 kHz

In summary, this research champions NDE findings via comparative exploration that the single most determining factor of NDE findings output, accuracy, and application is transducer frequency. Frequency dictates what data will be most reliable and impactful. The data that was received most reliably and impactfully at 54 kHz is an overarching perspective of macro-degradation that clearly and definitively determines whether samples are largely decayed or sufficiently protected; simultaneously, the data most reliably and impactfully received at 250 and 500 kHz is a higher spatial resolution that facilitates the qualitative assessment of ideal AER doses for identification and the quantitative assessment of better micro-damage development differentiation over the frozen-thaw cycles.

Ultimately, these results justify a multi-frequency ultrasonic test for an NDE approach to concrete durability, as frequency variations allow for a comprehensive understanding to mesh generalized degradation trends with findings that are more specific to localized damage for a better thorough understanding of concrete performance. The more confident one can be about durability assessments, the longer anticipated service life predictions will be, especially for performance mixes with complex designs expected for use in cold weather applications.

4. Conclusion

Casting and evaluation of four cylindrical concrete specimens were performed using the Ultrasonic Pulse Velocity (UPV) method. Three pairs of transducers with nominal frequencies of 54 kHz, 250 kHz, and 500 kHz, respectively, were used. Each concrete mix was prepared with four concentrations of air-entraining agent (0%, 0.1%, 0.125%, and 0.25%) to determine whether or not the microstructure would crack under freeze-thaw cycling. Specimens were subjected to artificially accelerated temperatures in a commercially-engineered freezer for eight weeks, echoing natural temperature fluctuations found in the field.

Results were assessed for sensitivity relative to wave velocity and wave attenuation as determined by UPV to assess internal damage. The findings indicate significant frequency dependence on wave attenuation in concrete mixes within this frequency range. For instance, the control specimen (0% AER) experienced maximum attenuation at 500 kHz (Aatt ≈ 17 dB), while attenuation dropped to ≈12 dB at 54 kHz and ≈14 dB at 250 kHz; Moreover, the attenuation from the control mix to the air-entraining dosage increased with frequency, for example, the 500 kHz transducer was better at assessing damage relative to microcracking/micro-debonding at the cement-aggregate interface (damage that likely smaller waves couldn't assess as effectively) since the relative changes from AER 0% to AER 0.25% were more apparent, indicating the transducer's sensitivity relative to earlier damage determination.

In addition, the comparative findings also assist in validating the presence of frequency-dependent variation within these non-destructive evaluations (NDE); where the 54 kHz NDE provided a more comprehensive degradation assessment, the higher frequencies, in particular the 250 kHz and 500 kHz provided better diagnostic resolution which clearer assessment of ideal air-entraining agent dosage levels and enhanced micro-structure evolution assessments considering freeze-thaw exposure.

Ultimately, these results validate the need for testing across multiple frequencies based on these results across multiple frequencies of ultrasonic testing with NDE for concrete durability assessment based on mixture design for cold weather. Testing across various frequencies will provide researchers with more comprehensive degradation assessments but more specific damage characteristics which will enhance the reliability of assessments and reduce error in service life determinations.

5. Declarations

5.1. Author Contributions

Conceptualization, S.H.F. and M.K.; methodology, S.H.F.; software, S.H.F.; validation, S.H.F., M.K., and Z.A.M.A.; formal analysis, S.H.F.; investigation, J.M.F. and S.H.; resources, J.M.F.; data curation, S.H.; writing—original draft preparation, S.H.F.; writing—review and editing, M.K. and Z.A.M.A.; visualization, S.H.F.; supervision, S.H.F.; project administration, S.H.F. All authors have read and agreed to the published version of the manuscript.

5.2. Data Availability Statement

The data presented in this study are available on request from the corresponding author.

5.3. Funding

The authors received no financial support for the research, authorship, and/or publication of this article.

5.4. Conflicts of Interest

The authors declare no conflict of interest.

6. References

[1] Sih, G. C., & Ditomasso, A. (2012). Fracture mechanics of concrete: Structural application and numerical calculation: Structural Application and Numerical Calculation. Springer Science & Business Media, Dordrecht, Germany. doi:10.1007/978-94-009-6152-4.

[2] Shields, Y., Garboczi, E., Weiss, J., & Farnam, Y. (2018). Freeze-thaw crack determination in cementitious materials using 3D X-ray computed tomography and acoustic emission. Cement and Concrete Composites, 89, 120–129. doi:10.1016/j.cemconcomp.2018.03.004.

[3] Fartosy, S. H., Abd, L. M., Kohees, M., & Abd Hacheem, Z. (2024). Ultrasonic characterization of damage induced by temperature variations in concrete medium treated with nanosilica. Magazine of Civil Engineering, 17(5), 12907. doi:10.34910/MCE.129.7.

[4] Puri, S., & Weiss, J. (2006). Assessment of Localized Damage in Concrete under Compression Using Acoustic Emission. Journal of Materials in Civil Engineering, 18(3), 325–333. doi:10.1061/(asce)0899-1561(2006)18:3(325).

[5] Neville, M. (2011). Properties of concrete. Pearson Education Limited, London, United Kingdom.

[6] Hadi, R. S., & Fadhil, H. S. (2021). the Mechanical Behavior of Polymer Composites Reinforced by Natural Materials. Journal of Engineering and Sustainable Development, 25(2), 88–96. doi:10.31272/jeasd.25.2.10.

[7] Fartosy, S. H., Abdalqadir, N. A., Al-Mussawy, H. A., Jafar, N. Q., & Ghosh, S. (2024). a Combined Ultrasonic Procedure to Evaluate Damage in Concrete Beams Subjected to Static Load. Journal of Engineering and Sustainable Development, 28(2), 213–221. doi:10.31272/jeasd.28.2.5.

[8] Yang, Z. (2004). Assessing cumulative damage in concrete and quantifying its influence on life cycle performance modeling (PhD Dissertation). Purdue University, West Lafayette, United States.

[9] Pour-Ghaz, M. (2011). Detecting damage in concrete using electrical methods and assessing moisture movement in cracked concrete. Ph.D. dissertation, Purdue University, West Lafayette, United States.

[10] Hwang, E., Kim, G., Choe, G., Yoon, M., Gucunski, N., & Nam, J. (2018). Evaluation of concrete degradation depending on heating conditions by ultrasonic pulse velocity. Construction and Building Materials, 171, 511–520. doi:10.1016/j.conbuildmat.2018.03.178.

[11] Fartosy, S., Gomez-Rodriguez, D., Cascante, G., Basu, D., & Dusseault, M. B. (2020). Effects of a fracture on ultrasonic wave velocity and attenuation in a homogeneous medium. Geotechnical Testing Journal, 43(2), 394–413. doi:10.1520/GTJ20180200.

[12] Bungey, J. H., & Millard, S. G. (1995). Testing of Concrete in Structures. CRC Press, Florida, Unted States. doi:10.4324/9780203487839.

[13] Abd, S. M., & Jassam, D. G. (2019). Improving Mechanical Properties of Lightweight Foamed Concrete Using Silica Fume and Fibers. Journal of Engineering and Sustainable Development, 23(2), 184–199. doi:10.31272/jeasd.23.2.14.

[14] Lencis, U., Udris, A., Kara De Maeijer, P., & Korjakins, A. (2024). Methodology for Determining the Correct Ultrasonic Pulse Velocity in Concrete. Buildings, 14(3), 720. doi:10.3390/buildings14030720.

[15] Santhanam, M. (2010). Ultrasonic characterization of damage in concrete. Structural Longevity, 3(1-2), 111-125.

[16] Zeng, Y., Meng, S., Xu, H., Yuan, S., Lang, W., & Chen, W. (2023). Strength attributes of fiber-reinforced lightweight aggregate concrete incorporating Lytag ceramsite under freeze-thaw environment. Journal of Building Engineering, 65. doi:10.1016/j.jobe.2022.105804.

[17] He, J., Serati, M., Veidt, M., & De Alwis, A. (2024). Determining rock crack stress thresholds using ultrasonic through-transmission measurements. International Journal of Coal Science and Technology, 11(1), 19. doi:10.1007/s40789-024-00669-x.

[18] Duan, A., Jin, W., & Qian, J. (2011). Effect of freeze-thaw cycles on the stress-strain curves of unconfined and confined concrete. Materials and Structures/Materiaux et Constructions, 44(7), 1309–1324. doi:10.1617/s11527-010-9702-9.

[19] Ensminger, D., & Bond, L. J. (2024). Ultrasonics: fundamentals, technologies, and applications. CRC Press, Florida, United States.

[20] Saboori, A. (2015). Application of damage mechanics to describe the behavior of concrete under fatigue and freeze-thaw processes. North Dakota State University, Fargo, United States.

[21] Zhang, K., Zhou, J., & Yin, Z. (2021). Experimental study on mechanical properties and pore structure deterioration of concrete under freeze–thaw cycles. Materials, 14(21), 6568. doi:10.3390/ma14216568.

[22] Wei, Y., Chen, X., Chai, J., & Qin, Y. (2024). Correlation between mechanical properties and pore structure deterioration of recycled concrete under sulfate freeze-thaw cycles: An experimental study. Construction and Building Materials, 412, 134794. doi:10.1016/j.conbuildmat.2023.134794.

[23] Hasan, M., Ueda, T., & Sato, Y. (2008). Stress-Strain Relationship of Frost-Damaged Concrete Subjected to Fatigue Loading. Journal of Materials in Civil Engineering, 20(1), 37–45. doi:10.1061/(asce)0899-1561(2008)20:1(37).

[24] Liu, M., & Wang, Y. (2012). Damage Constitutive Model of Fly Ash Concrete under Freeze-Thaw Cycles. Journal of Materials in Civil Engineering, 24(9), 1165–1174. doi:10.1061/(asce)mt.1943-5533.0000491.

[25] Gök, K. (2025). Influence of concrete near-surface damage to ultrasonic pulse velocity testing (M.Sc. Thesis). Delft University of Technology, Delft, Netherlands.

[26] Zalegowski, K. (2025). Pore Structure Influence on Properties of Air-Entrained Concrete. Materials, 18(12), 2885. doi:10.3390/ma18122885.

[27] Wu, H., Lv, C., Xu, Y., Sun, Y., Qu, S., & Zhou, X. (2025). Deterioration of Concrete Under the Combined Action of Sulfate Attack and Freeze–Thaw Cycles: A Review. Materials, 18(18), 4309. doi:10.3390/ma18184309.

[28] Lin, H., Han, Y., Liang, S., Gong, F., Han, S., Shi, C., & Feng, P. (2022). Effects of low temperatures and cryogenic freeze-thaw cycles on concrete mechanical properties: A literature review. Construction and Building Materials, 345, 128287. doi:10.1016/j.conbuildmat.2022.128287.

[29] Shang, H. shuai, & Song, Y. pu. (2008). Behavior of air-entrained concrete under the compression with constant confined stress after freeze-thaw cycles. Cement and Concrete Composites, 30(9), 854–860. doi:10.1016/j.cemconcomp.2007.10.006.

[30] Slawinski, M. A. (2020). Waves and rays in elastic continua: Fourth edition. World Scientific Publishing, Singapore. doi:10.1142/11994.

[31] ACI 211-91. (2002). Standard practice for selecting proportions for normal, heavyweight, and mass concrete. Concrete (Issue Reapproved 2009, 1–38. American Concrete Institute, Farmington Hills, United States.

[32] Krautkra¨mer, J., Krautkra¨mer, H., & Sachse, W. (1984). Ultrasonic Testing of Materials. Journal of Applied Mechanics, 51(1), 225–225. doi:10.1115/1.3167589.

[33] Kirlangic, S. (2013). Condition assessment of cemented materials using ultrasonic surface waves. Ph.D. Dissertation, University of Waterloo, Waterloo, Canada.